Advanced Composite Materials
Publication details, including instructions for authors and subscription information:
http://www.tandfonline.com/loi/tacm20

Initiation and Growth Behavior of Small Surface Fatigue Cracks on SiC Particle-Reinforced Aluminum Composites

Sang-Hyoup Lee [a], Young-Geun Choi [b] & Sang-Tae Kim [c]
[a] Division of Automobile Industries, Gumi College, Gumi 730-711, S. Korea
[b] Division of Automobile Industries, Gumi College, Gumi 730-711, S. Korea
[c] School of Mechanical Engineering, Yeungnam University, Gyongsan 712-749, S. Korea
Version of record first published: 02 Apr 2012.

To cite this article: Sang-Hyoup Lee , Young-Geun Choi & Sang-Tae Kim (2010): Initiation and Growth Behavior of Small Surface Fatigue Cracks on SiC Particle-Reinforced Aluminum Composites, Advanced Composite Materials, 19:4, 317-330

To link to this article: http://dx.doi.org/10.1163/092430409X12605406698435

VSP

Advanced Composite Materials 19 (2010) 317–330

ADVANCED COMPOSITE MATERIALS
brill.nl/acm

Initiation and Growth Behavior of Small Surface Fatigue Cracks on SiC Particle-Reinforced Aluminum Composites

Sang-Hyoup Lee [a], **Young-Geun Choi** [a] **and Sang-Tae Kim** [b,*]

[a] Division of Automobile Industries, Gumi College, Gumi 730-711, S. Korea
[b] School of Mechanical Engineering, Yeungnam University, Gyongsan 712-749, S. Korea

Received 2 March 2009; accepted 1 September 2009

Abstract
Reversed plane bending fatigue tests were conducted on SiC particle-reinforced aluminum composites. The initiation and growth behaviors of small surface fatigue cracks were continuously monitored by the replica technique and investigated in detail. The fatigue life of MMC is shorter than that of matrix because there exists interface debonding of SiC particles and matrix on the whole face of the notch part in the casting metal matrix composite (MMC). The coalescence of small cracks was observed in the surface after conducting fatigue tests at high stress levels. Due to the coalescence, a higher crack growth rate of small cracks rather than that of long cracks was recognized in $da/dn - K_{max}$ relationship.

Keywords
SiC particle, fatigue, crack initiation, crack growth, small surface crack, bending fatigue test, metal matrix composite

1. Introduction

Nowadays, when machine structures are operated in more extreme conditions, new materials are developed to meet these conditions quickly. Metal matrix composites (MMCs) are examples of such materials and contain ceramic reinforcement phases with high strength and high elasticity. Therefore, MMCs have higher specific elasticity, higher specific strength, better heat resistance, and wear resistance than metals without reinforcement. These materials are widely used as light structural materials and functional materials in the field of aerodynamic, aerospace, and defense industries and automobile manufacture [1–3]. The composites of aluminum matrix with discontinuous SiC fibers are more widely used than composites of alu-

* To whom correspondence should be addressed. E-mail: stkim@ynu.ac.kr
Edited by the KSCM

DOI:10.1163/092430409X12605406698435

minum matrix with long continuous SiC fibers because they can be easily fabricated in the same metallurgical processing method as aluminum alloys with low costs.

Discontinuous SiC fibers can be prepared in two types: as whiskers and particles. Whisker type fibers have the better mechanical properties but incur higher manufacturing costs. The particle-reinforced composites have been more actively studied than the fiber-reinforced composites because of lower costs [4–8]. MMCs in practical use should have better fatigue characteristics, corrosion resistance, environmental resistance and thermal cyclic characteristics in order to be used widely as structural materials. Among those properties, the excellent fatigue resistance is perhaps the most important property required for structural materials. Fatigue crack propagation rate, da/dn, can be expressed as a linear function of stress intensity factor, ΔK, in Paris' equation. If crack tip closure behavior is considered as Elber indicated, the effective stress intensity factor, ΔK_{eff} can be the most effective governing parameter when the crack is opening [9, 10].

Shang and Ritchie showed that composites with coarse SiC particles have high crack closure level and resistance to crack propagation because of crack tip shielding by roughness-induced crack closure in long crack propagation. However, when the ΔK_{eff} with the effect of crack closure was considered, composites with fine SiC particles showed high resistance to crack propagation [11]. Kobayashi *et al.* measured the crack closure in particle-reinforced composites with the compliance method and found that the crack closure in low ΔK and near the ΔK_{th} region was due to the surface roughness-induced crack closure and the oxide particle-induced crack closure, and the crack closure in low ΔK came from the plasticity-induced crack closure [12]. Other experimental results for the long crack propagation behavior in MMCs can be found elsewhere [13–15]. However, in practice, small surface cracks from surface defects give rise to more damages than the long through cracks in real structures. The small surface cracks propagate in the region below ΔK_{th} and propagate more quickly than long cracks in same ΔK region [16–18]. According to the study of SiC particle-reinforced Al alloys, the small surface cracks were initiated from the interfaces between SiC particles and Al matrix. Cracks stopped at the interfaces of SiC particles in the low ΔK region and cracks did not stop in the high ΔK region [8]. Even though some results about the initiation and propagation behavior of small surface cracks in MMCs can be found elsewhere, it is not sufficient for the understanding of fatigue failure and the reliability establishment of MMCs [19–22]. In this study, to find out the initiation and growth behavior of small surface cracks in SiC particle-reinforced composites fabricated by molten casting, plane bending fatigue tests were employed and cracks were continuously monitored with the replica method. After fatigue tests, the fracture surfaces were observed with the scanning electron microscope.

2. Experimental Details

2.1. Test Specimens and Test Apparatus

The material used in this study was the composite material with matrix of molten cast Al–Si–Mg alloy, Al6061-T6 and SiC particles of 20% volume fraction, which were developed by the ALCAN Company in Canada. The composition and mechanical properties of material are shown in Tables 1 and 2, respectively. Figure 1 shows the microstructure of the material after etching taken by optical microscope. Al particles with 50–100 μm diameters appeared in white color and the mixed phases of Al matrix and SiC particles of 10–30 μm diameters can be seen around the white Al particles. From these materials, specimens with the length of 50 mm, width of 12 mm, an elliptical notch with major axis length of 6 mm, minor axis length of 3 mm and depth of 0.3 mm were machined for the fatigue crack growth tests. The specimen geometry adapted in this study is shown in Fig. 2. Fatigue tests were conducted on a small coin-shaped plane bending fatigue test machine.

2.2. Experimental Procedures

All fatigue tests were conducted using a small coin-shaped plane bending fatigue machine. All tests were done with the completely reversed constant amplitude loading with a frequency of 30 Hz. The small surface crack length was measured with the optical microscope from the replicas taken periodically in the vicinity of the notch, 4 mm × 8 mm area. The fractured surfaces after fatigue tests were observed on the scanning electron microscope. In this study, the crack initiation life, N_i, and fatigue fracture life, N_f, are defined as the cycle numbers of total crack length $2a = 0.2$ mm and $2a = 2.0$ mm, respectively. The stress intensity factor, K, was calculated with the crack length in the projected plane vertical to loading axis. Newman–Raju equation was used in this calculation [21].

Table 1.
The chemical compositions of matrix material (wt%)

Si	Fe	Cu	Mn	Mg	Zn	Cr	Ti	B	Ni	V	Ga	Al
0.834	0.262	0.306	0.01	1.263	0.003	0.107	0.20	0.002	0.01	0.01	0.02	Bal.

Table 2.
The mechanical properties of matrix and composite materials

Materials and matrix	2% proof stress $\sigma_{0.2}$ (MPa)	Tensile strength σ_b (MPa)	Elongation δ (%)	Young's modulus E (GPa)
A6061-T6	346	365	16.0	66.9
SiC_p/A6061-T6	407	460	3.6	103

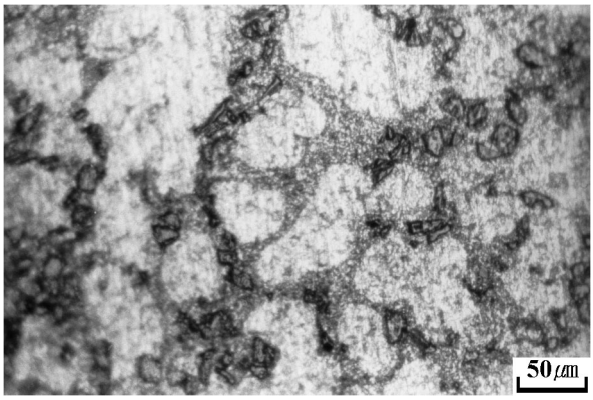

Figure 1. Microstructure of SiC particle-reinforced Al composites.

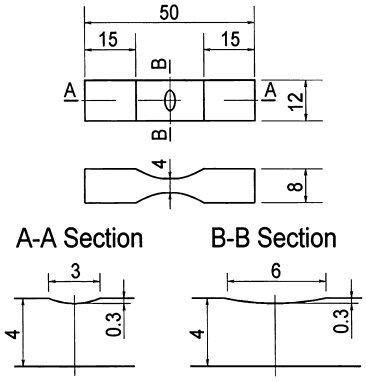

Figure 2. Test specimen configuration (units: mm).

3. Results and Discussion

3.1. S–N Curves

Figure 3 shows S–N curves with the crack initiation life and fatigue fracture life *versus* stress amplitude, where the stress concentration factor was determined as 1.67 from the finite element method. In the figure, the open circle (○) represents the crack initiation life and the closed circle (●) means the fatigue fracture life. Fracture life shows some data scatterings; however, the crack initiation life can be drawn on one line. For comparison, the crack initiation life (○) and the fatigue fracture life (▲) of Al6061 alloys were expressed in the same figure. It shows that SiC particle-reinforced MMC has higher fatigue strength than Al matrix material.

3.2. Fatigue Crack Initiation Pattern

Figure 4 depicts the positions for crack observation, A, B and C on the specimen. Figure 5 shows SEM photographs of the near-notch part of the specimen after repeating 3.2×10^5 cycles at a low stress level of $\sigma_a = 140$ MPa. In the figure,

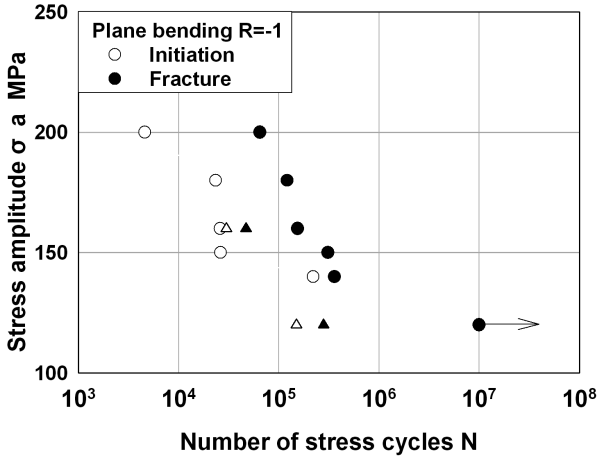

Figure 3. S–N curves for SiC particle-reinforced Al composites.

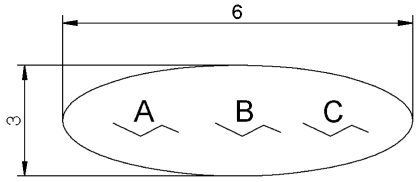

Figure 4. Example of observation of crack initiation.

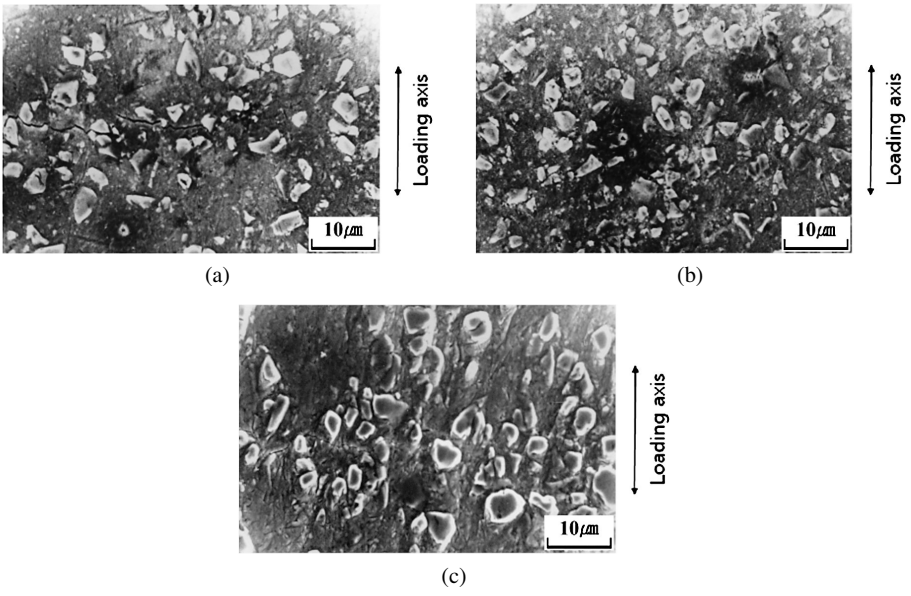

Figure 5. SEM photographs of near-notch part of specimen after repeating 3.2×10^5 cycles at a low stress level of $\sigma_a = 140$ MPa in SiC_p/Al composites: (a) Point A in the near-notch part of specimen; (b) point B in the near-notch part of specimen; (c) point C in the near-notch part of specimen.

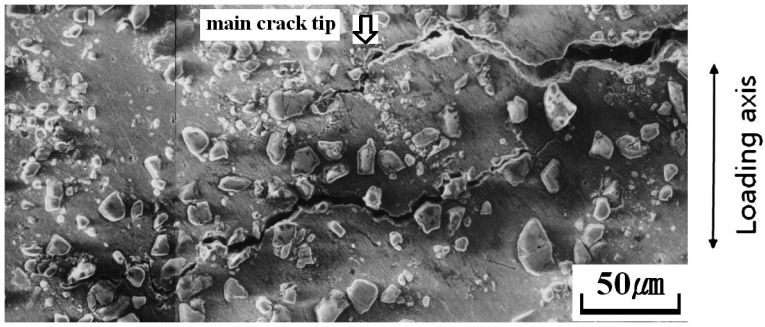

Figure 6. SEM photograph of near-notch part of specimen after repeating 3.7×10^4 cycles at a high stress level of $\sigma_a = 180$ MPa in SiC_p/Al composites.

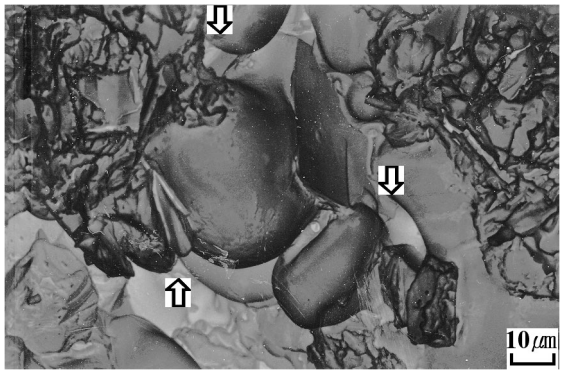

Figure 7. SEM photograph depicting the crack initiation points in SiC_p/Al composites.

photographs 5(a), 5(b), and 5(c) correspond to A, B and C in the near-notch part of the specimen. It can be seen that cracks were initiated in the near-notch part of the specimen at low stress level. Figure 6 shows SEM photographs of the near-notch part of the specimen after repeating 3.7×10^4 cycles at a high stress level of $\sigma_a = 180$ MPa. In Fig. 6, many small arrested-cracks with main crack were observed. These cracks after initiation were grown up to ~40 μm and stopped. The crack was initiated at the defect made by a parting of an SiC particle from the matrix and merged to main crack. As shown in the SEM photograph of Fig. 7, there are many crack initiation points from the interface debonding between SiC particles and matrix metal. It was caused by high extrusion ratio during the manufacturing process and reduced the fatigue strength.

3.3. Small Fatigue Cracks and Crack Propagation Curves

Figure 8 is an example of continuous observation of small fatigue cracks at low stress level of $\sigma_a = 150$ MPa by replica method. As can be seen, small cracks developed after 26 149 cycles at the stress level of $\sigma_a = 150$ MPa (Fig. 8(a)). Every crack merged into two cracks and finally made one main crack. All the cracks in the

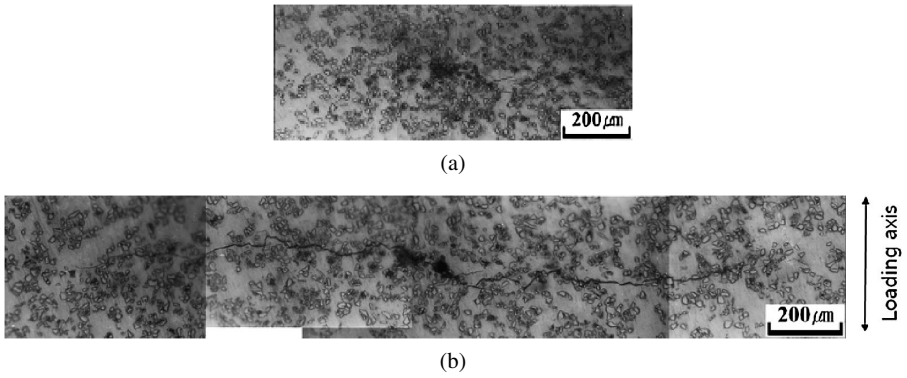

Figure 8. Successive observation of crack growth behavior in SiC_p/Al composites ($\sigma_a = 150$ MPa): (a) 2.61×10^4 cycles; (b) 3.09×10^5 cycles.

figure repeat very small flexions microscopically; however, the direction of crack growth is vertical to the loading direction macroscopically. Several cracks grow and merge to one crack with near cracks in high stress level and cracks in different propagating directions stop at the crack tip. Figure 9 is an example of continuous observation of small fatigue cracks at the stress level of $\sigma_a = 200$ MPa. Initial small cracks developed after 4062 cycles (Fig. 9(a)) and coalesced into one crack (Fig. 9(b)). The crack propagation pattern at high stress level is the same as that at low stress level. Two or three cracks developed and merged to one crack after growth vertically to the loading direction at high stress level and at low stress level. Figures 10–12 show the fatigue crack propagation curves. Crack length, $2a$, is the projected length vertical to the loading direction and the dashed line in the figure means coalescence of cracks.

Figure 10 shows crack growth curve at the stress level of $\sigma_a = 150$ MPa. In this figure, several cracks developed at low stress level and merged to one crack. Coalescence of the main crack and small cracks increase the crack length and make the discontinuous crack growth curves. However, some cracks show the lower crack growth rates after coalescence, because cracks after coalescence grow in the depth direction of the specimen and the cracks observed on the surface do not grow thoroughly. Figure 11 is the crack growth curve at the stress level of $\sigma_a = 200$ MPa. The crack length increases rapidly in the slant direction to the loading axis at the beginning and then cracks repeat the stopping and growing occasionally at several places. After the coalescence of the main crack and small cracks, the crack length increased and all data were put in one line. Figure 12 shows crack growth curves at the stress levels of $\sigma_a = 140$ MPa, $\sigma_a = 150$ MPa, $\sigma_a = 160$ MPa, $\sigma_a = 180$ MPa and $\sigma_a = 200$ MPa, respectively. Crack growth patterns are very similar to the curves described previously.

3.4. Small Crack Growth Patterns and Fractography

Crack growth paths in the surface of specimens were observed in detail by scanning electron microscopy (SEM). Figure 13 shows an example of crack growth observa-

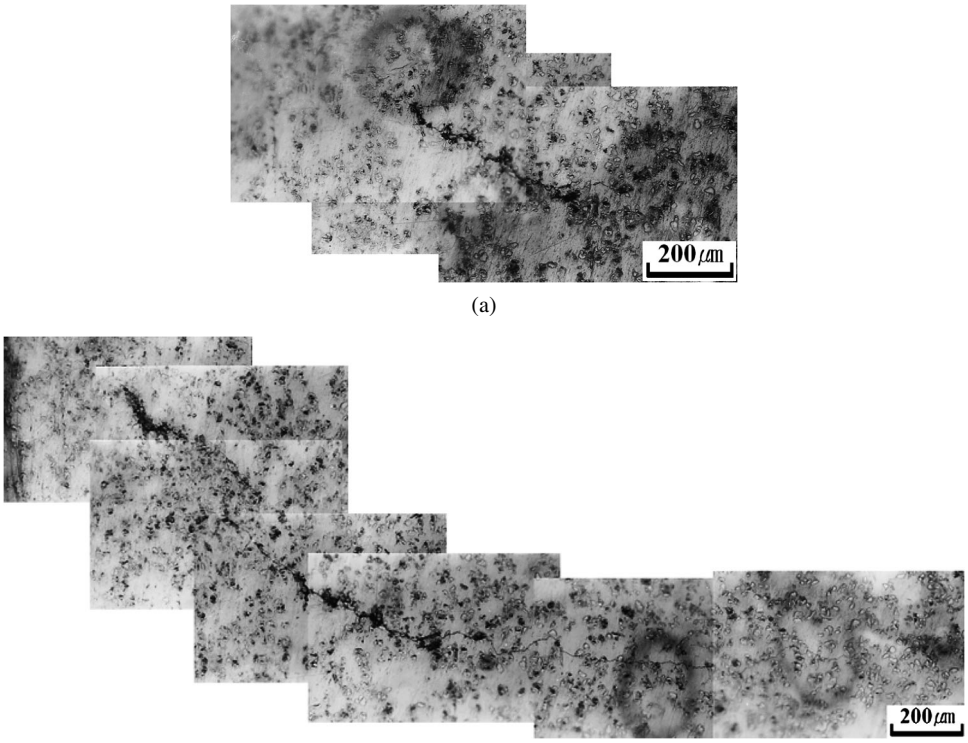

Figure 9. Successive observation of crack growth behavior in SiC_p/Al composites ($\sigma_a = 200$ MPa): (a) 0.46×10^4 cycles; (b) 4.64×10^4 cycles.

tion at the fatigue crack tip in low K_{max} region ($K_{max} = 1.51$–2.09 MPa $m^{1/2}$) with $\sigma_a = 140$ MPa. Several cracks with a few tens of μm developed at a short distance from the notch tip and propagated independently until they finally joined together. After that, the crack growth behavior is similar to crack growth at the high stress level. However, the micro-cracks, which develop into the relatively long lengths, or cracks, which do not merge into the main crack, are not identified at low stress level, as shown in Fig. 13. The distance between main crack and small cracks is ~25 μm. Figure 14 shows the crack growth paths at the fatigue crack tip in high K_{max} region ($K_{max} = 6.39$–6.53 MPa $m^{1/2}$) with $\sigma_a = 200$ MPa. It can be observed that the initiation of the same types of micro-cracks and merging to main crack are similar to those at low stress level. Especially, it shows the initiation of micro-cracks including the fracture of SiC particles without initial defects. Several bridgings in both the high and low K_{max} region were identified (arrow D in Fig. 14(a)).

These bridgings were remaining in all the regions from crack tip to the rear and the number of bridgings increased in the approach to the crack tip. The cracks were propagated into the matrix materials or along the interfaces between SiC particles and matrix materials. Mostly the cracks propagate by avoiding SiC particles (arrow

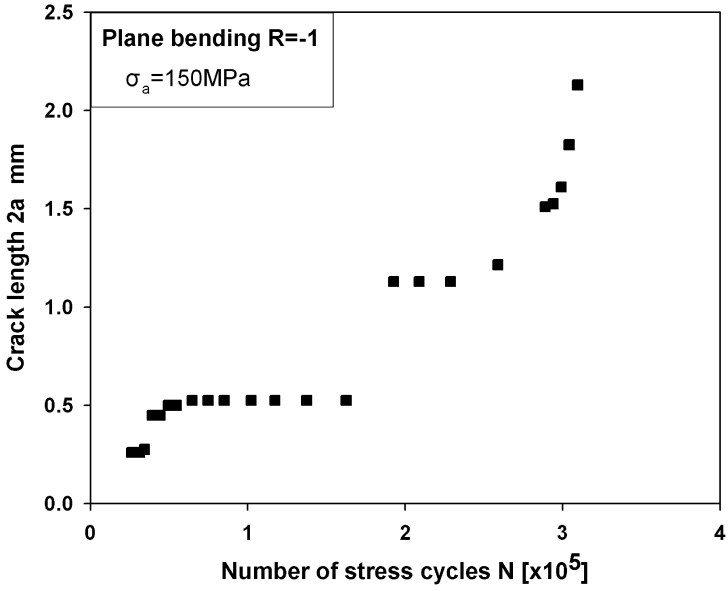

Figure 10. Crack growth curves in SiC_p/Al composites ($\sigma_a = 150$ MPa).

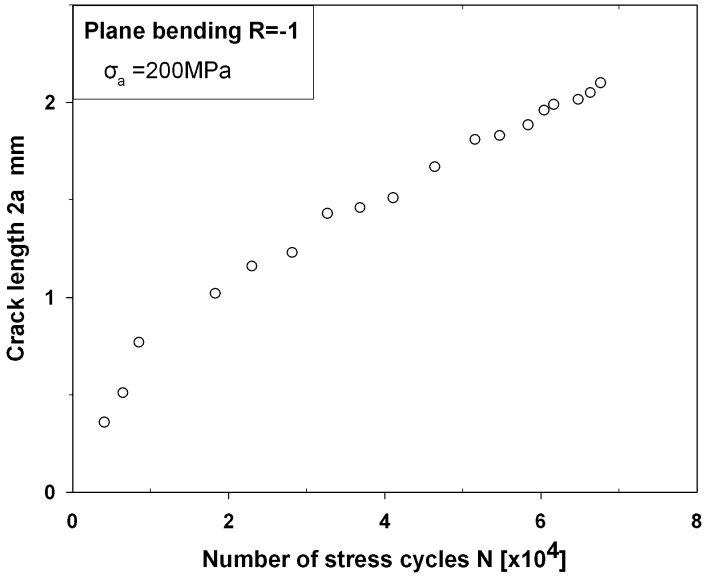

Figure 11. Crack growth curves in SiC_p/Al composites ($\sigma_a = 200$ MPa).

A in Fig. 14(b)). Micro-cracks of approximately 10 μm developed near the main crack tip in the main crack plane in high K_{max} region ($2a = 1.02$ mm; $N = 1.82 \times 10^4$ cycles) and joined with cracks in the other plane after 1000 cycles. SiC particle (indicated as A in Fig. 14(b)) with initial defect becomes the crack growth path. As

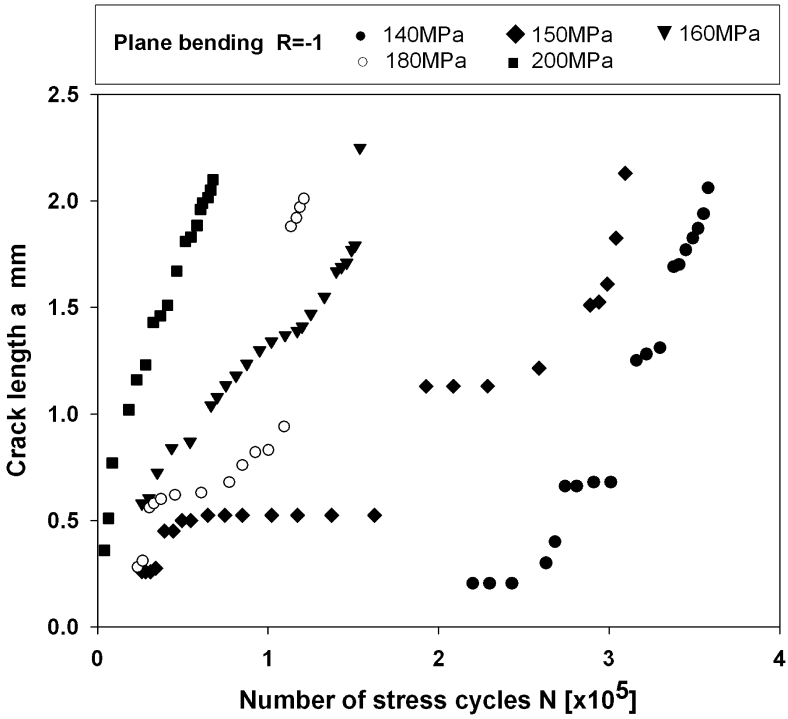

Figure 12. Crack growth curves in SiC_p/Al composites with different stress levels.

shown in Fig. 14(b), some cracks cut through the SiC particles without making any defects and propagated.

Figure 15 is SEM photograph showing the macroscopic surface fractured at high stress level, $\sigma_a = 200$ MPa. This is the fatigue fracture surface of which two fatigue cracks joined together and each fracture surface has a semi-circular pattern. As indicated with an arrow in the figure, there are two large discontinuities. These are due to the coalescence or the overlapping of three cracks. For comparison, the fracture surface of matrix material Al6061-T6 is shown in Fig. 16. Two cracks developed and propagated at this stress level and made one fracture surface with joining two fracture surfaces together. Each fracture surface shows a semi-circular pattern with aspect ratio, λ $(= c/a)$ of approximately 0.56: here a is surface crack length and c is thickness-through crack length.

3.5. $\mathrm{d}a/\mathrm{d}n - K_{\max}$ *Relationship*

Figure 17 shows the $\mathrm{d}a/\mathrm{d}n - K_{\max}$ relationship for small surface cracks. At low stress level, there are some scatterings in crack growth rates due to the initiation of many cracks, some of which join together. At high stress level, meanwhile, it shows the relatively small scatterings. Even though the small cracks are propagating by repeating the initiation and coalescence of small cracks, the length of small cracks

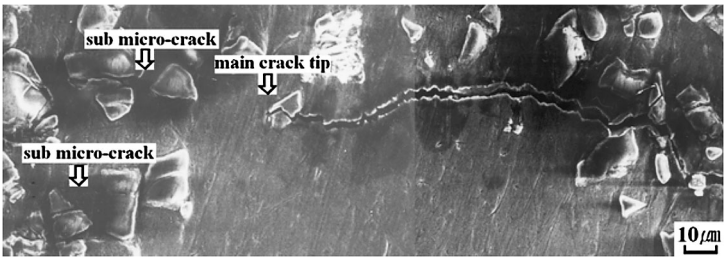

(a)

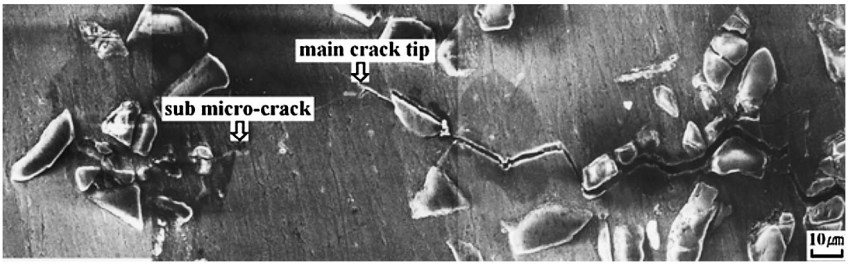

(b)

Figure 13. The details of fatigue crack growth path in SiC_p/Al composites ($\sigma_a = 140$ MPa): (a) $N = 2.6 \times 10^5$ cycles, $2a = 0.40$ mm, $K_{max} = 2.09$ MPa $m^{1/2}$; (b) $N = 3.30 \times 10^5$ cycles, $2a = 1.31$ mm, $K_{max} = 3.70$ MPa $m^{1/2}$.

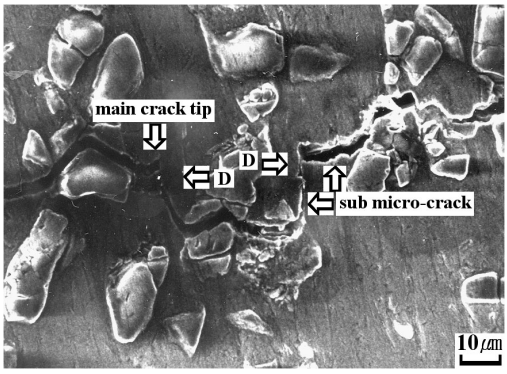

(a)

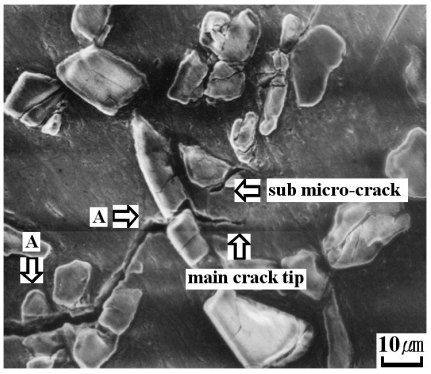

(b)

Figure 14. The details of fatigue crack growth path in SiC_p/Al composites ($\sigma_a = 200$ MPa): (a) $N = 1.82 \times 10^4$ cycles, $2a = 1.02$ mm, $K_{max} = 4.69$ MPa $m^{1/2}$; (b) $N = 6.47 \times 10^4$ cycles, $2a = 2.01$ mm, $K_{max} = 6.47$ MPa $m^{1/2}$.

is shorter than that of the main crack and the other crack growth data are in the acceptable scattering range.

Generally, the small cracks are propagating faster than the long cracks at the same ΔK level and even propagating in lower ΔK_{th} values. For the long cracks, plasticity-induced crack closure, oxide particle-induced crack closure, or fracture surface roughness-induced crack closure can be employed to explain the growth

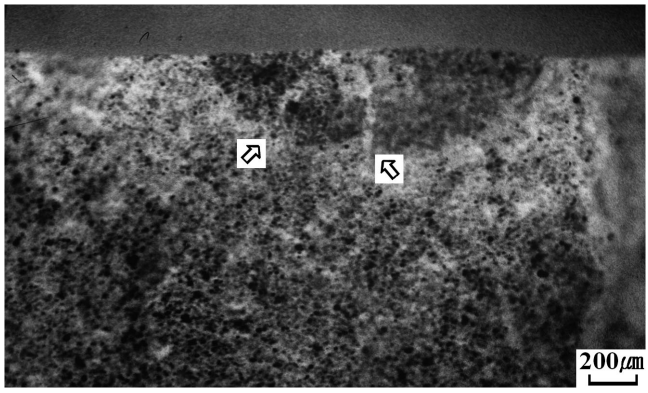

Figure 15. SEM photograph of fracture surface in SiC_p/Al composites ($\sigma_a = 200$ MPa).

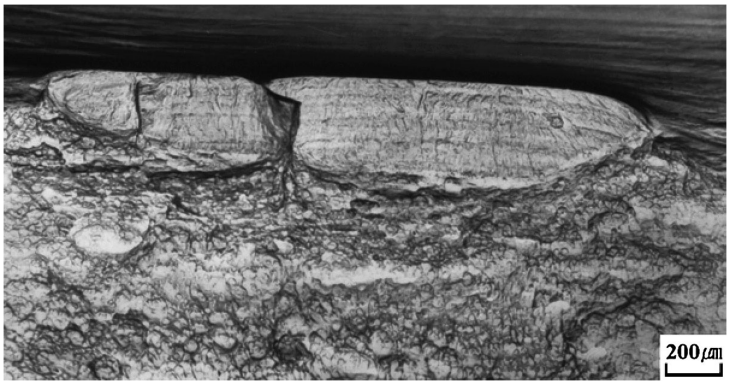

Figure 16. SEM photograph of fracture surface of Al matrix ($\sigma_a = 120$ MPa).

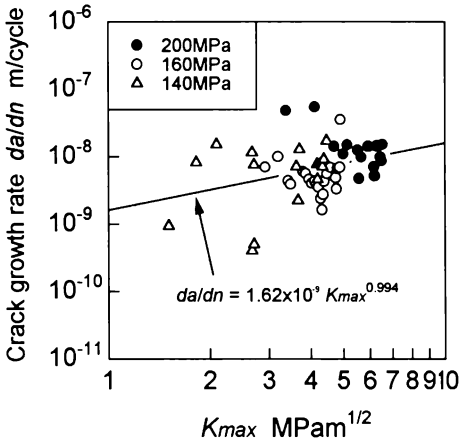

Figure 17. $da/dn - K_{max}$ relation for SiC_p/Al composites.

behavior. In the case of small cracks, the cracks are closed in all tensile loading conditions and the crack closure effect is negligible. The shielding in crack tip wake by crack deflection or bridging is affecting in the growth behavior of small cracks. The growth rate of small cracks is affected by the obstruction of SiC particles in low stress level and is higher than that of long cracks.

4. Conclusions

Reversed plane bending fatigue tests were conducted on SiC particle-reinforced aluminum 6061-T6 composites. The initiation and growth behaviors of small surface fatigue cracks were continuously monitored by the replica technique and SEM observation. The results in this study are summarized in the following.

1. The fatigue life data for SiC reinforced Al composites can be drawn on one S–N curve and show that SiC particle-reinforced MMCs have the higher fatigue strength than Al matrix material in the crack initiation stage.
   The fatigue life of MMC is shorter than that of the matrix because there exists interface debonding of SiC particles and matrix on the whole face of the notch part in the casting metal matrix composite (MMC). The coalescence of micro-cracks was observed in the tests conducted at high stress levels. Due to the coalescence, a higher crack growth rate of small cracks rather than that of long cracks was recognized in the $da/dn - K_{max}$ relationship.
2. The small cracks were initiated and propagated at the near notch part of specimens regardless of stress level. The crack initiation points were identified as the defects made by detachment of SiC particle from the matrix, the interfaces between the matrix and SiC particles, or the places where SiC particles were broken.
3. The fatigue cracks were propagated into the matrix materials or along the interfaces between SiC particles and matrix materials. During the crack growth, the micro-cracks in the crack growth path were merged into the main crack. These micro-cracks were initiated and stopped by cyclic loading regardless of high stress field at the main crack tip.
4. There are some scatterings in the $da/dn - K_{max}$ relationship at low stress level. These were caused by the initiation of many cracks and joining together. In high stress level, meanwhile, it shows the relatively small scatterings.

Acknowledgement

This research was supported by the Yeungnam University research grants in 2007.

References

1. K. S. Han and Y. H. Kim, Processing and application of metal matrix composite materials, *J. KSME* **32**, 46–56 (1992).
2. S. N. Ahmad, J. Hashim and M. I. Ghazali, The effects of porosity on mechanical properties of cast discontinuous reinforced metal–matrix composite, *J. Compos. Mater.* **39**, 451–466 (2005).
3. Y. C. Park, Y. J. Jo, S. H. Baek and Y. Furuya, Fatigue design curve of a TiNi/Al shape memory alloy composite for aircraft stringer design, *Smart Mater. Struct.* **18**, 055009 (2009).
4. M. Dutta, G. Bruno, L. Edwards and M. E. Fitzpatrick, Neutron diffraction measurement of the internal stresses following heat treatment of a plastically deformed Al/SiC particulate metal–matrix composite, *Acta Mater.* **52**, 3881–3888 (2004).
5. S. K. Woo and I. S. Han, Technology trend and prospect of silicon carbide based ceramics for energy and environment application, *Ceramicist* **10**, 23–30 (2007).
6. A. Sugeta, M. Jono, K. Bessho and A. Sakaguti, Initiation and growth behavior of small surface fatigue crack on SiC particle-reinforced aluminum composites, *J. Soc. Mater. Sci. Japan* **45**, 443–448 (1996).
7. C. Tekmen and U. Cocen, The effect of Si and Mg on age hardening behavior of Al–SiC_p composites, *J. Compos. Mater.* **37**, 1791–1800 (2003).
8. S. Kumai, J. E. King and J. F. Knott, Fatigue crack growth in SiC particulate-reinforced aluminum alloys, *Fatigue'90* **II**, 869–874 (1990).
9. P. Paris and F. Erdogan, A critical analysis of crack propagation laws, *Trans. ASME, Ser. D* **85**, 528–533 (1963).
10. W. Elber, The significance of fatigue crack closure, *ASTM STP* **486**, 230–242 (1971).
11. J. K. Shang and R. O. Ritchie, On the particle-size dependence of fatigue crack propagation thresholds in SiC-particulate-reinforced aluminum-alloy composites: role of crack closure and crack trapping, *Acta Metall. Mater.* **37**, 2267–2278 (1989).
12. T. Kobayashi, H. Iwanari, S. Hakamata, M. Niinomi and H. Toda, Fatigue crack propagation characteristics in SiCp/6061-T6 composite, *J. Japan Inst. Metals* **55**, 72–78 (1991).
13. A. F. Whitehouse and T. W. Clyne, Cavity formation during tensile stringing of particulate and short fiber metal matrix composites, *Acta Metall. Mater.* **41**, 1701–1711 (1993).
14. N. Koiso, H. Misawa and S. Kodama, Fatigue propagation of aluminum alloy reinforced by SiC particles, *J. Soc. Mater. Sci. Japan* **38**, 1206–1211 (1989).
15. S. B. Biner, Growth of fatigue cracks emanating from notches in SiC particulate aluminum composite, *Fatigue Fract. Engng Mater. Struct.* **13**, 637–646 (1990).
16. E. R. de los Rios, Z. Tang and K. J. Miller, Short crack fatigue behavior in a medium carbon steel, *Fatigue Fract. Engng Mater. Struct.* **7**, 97–108 (1984).
17. M. H. El Haddad, K. N. Smith and T. H. Topper, Fatigue crack propagation of short cracks, *ASME J. Engng Mater. Technol.* **101**, 42–46 (1979).
18. J. Lankford, The growth of long fatigue crack growth in a SiC reinforced aluminum alloy, *Fatigue Fract. Engng Mater. Struct.* **5**, 233–248 (1982).
19. J. K. Shang and R. O. Ritchie, Crack bridging by uncracked ligaments during fatigue-crack growth in SiC-reinforced aluminum-alloy composites, *Metall. Trans. A* **20**, 897–908 (1989).
20. C. Masusa and Y. Tanaka, Fatigue fracture mechanisms for SiC whiskers and SiC particulates aluminum composites, *Iron and Steel (Tetsu to Kou in Japanese)* **75**, 1753–1760 (1989).
21. J. C. Newman and I. S. Raju, Stress intensity factor equations for cracks in three-dimensional finite bodies, *ASTM STP* **791**, 238–265 (1983).
22. N. Kawagoishi, H. Nisitani and T. Tsuno, Effect of heat treatments on the fatigue crack growth properties of an aluminum casting alloy, *Trans. Japan Soc. Mech. Engng* **55**, 1733–1739 (1991).